Inclusion of Rotor Dynamics in Controller Design for Helicopters

W. E. Hall Jr.* and A. E. Bryson Jr.†
Stanford University, Stanford, Calif.

State-feedback-controllers and state-estimators (filters) are designed for the roll-pitch-horizontal motions of a helicopter near hover, using a new quadratic synthesis technique. One model (tenth order) uses a dynamic model of the rotor, whereas the other model (sixth order) assumes the rotor can be tilted instantaneously. It is shown that, for tight control, neglecting the rotor dynamics in designing the autopilot can produce unstable closed-loop response on the model that includes rotor dynamics. Two filters are designed to use only fuselage sensors and two are designed to use both fuselage and rotor sensors. It is shown that rotor states can be estimated with sufficient accuracy using only fuselage sensors so that it does not seem worthwhile to use rotor sensors. The mean square response of the vehicle to a gusty, random wind, using several different filter/state-feedback compensators, is shown to be satisfactory.

Nomenclature

A = matrix of state weighting coefficients (i.e., weighting of $\theta_F = A_{\theta F}$)
C = matrix of control gains
F = open loop (controls fixed) dynamics matrix
G = control distribution matrix
H = measurement distribution matrix
K = matrix of Kalman filter gains
P = covariance matrix of error estimate
Q = spectral density matrix of process noise
R = spectral density matrix of measurement noise
X = mean square response matrix of state responses
$\hat{X}$ = mean square response matrix of state estimates
p = roll rate
q = pitch rate
u,v = longitudinal and lateral velocities of vehicle center of mass
$\mathbf{u}$ = control vector
$\mathbf{w}$ = wind vector
θ = pitch angle
θ_c = lateral cyclic pitch
θ_s = longitudinal cyclic pitch
τ_c = correlation time of wind
φ = roll angle
Γ = process noise distribution matrix

Subscripts

$()_R$ = rotor state
$()_F$ = fuselage state

Superscripts

$()'$ = matrix of augmented system
$()^T$ = matrix transpose (rows and columns interchanged)
$\hat{()}$ = estimated state
$\tilde{()}$ = error in estimated state

Introduction

THE ability to hold attitude and to hover over a particular point in the presence of winds is a requirement common to most rotary-wing VTOL aircraft. The primary objective of a hover autopilot is to aid the pilot in accomplishing these tasks.

The technique of quadratic synthesis has recently been applied to designing hover controllers,[1,2] using a vehicle model which assumes instantaneous rotor tilting and perfect information on vehicle attitude, attitude rate, and velocity. In this paper, we consider the effect of rotor dynamics on hover autopilots and show that, for very tight control, rotor dynamics should be included in designing such controllers. We also consider the effect of sensor noise on such controllers.

In order to consider the effects of rotor dynamics and sensor noise, we developed a quadratic synthesis program that was faster and more accurate than the ones currently available.[3] This program, which we call OPTSYS (for Optimum Systems Synthesis[4]) uses the MacFarlane-Potter concept of eigenvector decomposition[5,6] instead of integrating matrix Riccati equations, and incorporates the very accurate QR algorithm of Francis[7] for determining the eigenvalues and eigenvectors of the Hamiltonian matrix. OPTSYS calculates a) the optimum state-feedback gains, b) the Kalman-Bucy filter gains, and c) the mean-square response of the controlled system to random inputs, all for the statistically stationary case. It is capable of handling very high order systems with many control inputs, disturbance inputs, and sensor measurements.

A Model of Roll-Pitch-Horizontal Velocity near Hover that Includes Rotor Dynamics

A two-rigid-body model of a typical rotary-wing VTOL aircraft near hover was derived in Ref. 8. The fuselage is regarded as one rigid body and the spinning rotor is modeled as another (axially symmetric) rigid body that can be tilted with respect to the fuselage by the controls, longitudinal and lateral cyclic pitch (see Fig. 1). This leads to a 16th order mathematical model since there are three translational degrees of freedom (DOF) for the mass center, three angular DOF for the fuselage, and two angular DOF for the rotor (assuming constant rotor spin velocity). If we disregard horizontal position of the mass center, the model reduces to 14th order; near hover, vertical motion and yaw motion are both virtually uncoupled, and the model reduces to one 10th-order system and two uncoupled 2nd-order systems (collective pitch controlling the vertical motion and tail rotor controlling the yaw motion).

Our attention here is focused on the 10th-order system. Using the results of many previous investigators for rotor-fuselage aerodynamic forces and torques,‡ we constructed

Presented as Paper 72-778 at the AIAA 4th Aircraft Design, Flight Test, and Operations Meeting, Los Angeles, Calif., August 7-9, 1972; submitted August 14, 1972; revision received January 5, 1973. This research was supported under NASA Contract NAS 2-5143 for the U. S. Army Air Mobility Research and Development Laboratory, Ames Directorate, NASA Ames Research Center, Moffett Field, Calif.

Index categories: VTOL Handling, Stability, and Control; Navigation, Control, and Guidance Theory.

*Postdoctoral Fellow, Stanford University; presently with Systems Control, Incorporated, Palo Alto, Calif. Associate Member AIAA.

†Professor and Chairman, Department of Aeronautics and Astronautics, Stanford University. Fellow AIAA.

‡The fuselage aerodynamic contributions are assumed to be negligible for this hover model.

Table 1 Elements of the open-loop dynamics matrix, the control distribution matrix, and the disturbance distribution matrix for a mathematical model of the Sikorsky S-61 Helicopter[a] (units are in ft, sec; angles in rad)

$$F = \begin{bmatrix} 0 & 0 & 1 & 0 & 0 & 0 & 0 & 0 & 0 & 0 \\ 0 & 0 & 0 & 1 & 0 & 0 & 0 & 0 & 0 & 0 \\ -41.3 & -601 & -30.2 & -42.6 & 0 & 0 & -30.4 & -50.1 & 0.126 & -0.284 \\ 599 & -56.7 & 42.6 & -29.4 & 0 & 0 & 50.2 & -30.2 & -0.283 & -0.122 \\ 0 & 0 & 0 & 0 & 0 & 0 & 1 & 0 & 0 & 0 \\ 0 & 0 & 0 & 0 & 0 & 0 & 0 & 1 & 0 & 0 \\ 4.97 & -0.94 & -0.044 & 0.0034 & 0 & 0 & -0.0521 & 0.0281 & 0.00124 & -0.00020 \\ 3.53 & 18.7 & -0.013 & -0.166 & 0 & 0 & -0.105 & -0.196 & -0.00076 & -0.00467 \\ -15.0 & 21.9 & 1.03 & -0.045 & -32.2 & 0 & 4.37 & 1.44 & -0.0166 & 0.0072 \\ 21.9 & 15.0 & -0.045 & -1.03 & 0 & 32.2 & 1.44 & -4.37 & -0.0072 & -0.0166 \end{bmatrix}$$

$$G^T = \begin{bmatrix} 0 & 0 & -601 & 5.52 & 0 & 0 & -0.938 & -4.97 & 21.8 & -16.8 \\ 0 & 0 & -1.47 & -599 & 0 & 0 & 1.32 & -3.52 & -16.8 & -21.8 \end{bmatrix}$$

$$\Gamma^T = \begin{bmatrix} 0 & 0 & 0.126 & -0.283 & 0 & 0 & 0.00124 & -0.00076 & -0.0166 & -0.0072 \\ 0 & 0 & -0.284 & -0.122 & 0 & 0 & -0.00020 & -0.00467 & 0.0072 & -0.0166 \end{bmatrix}$$

Open-loop eigenvalues are (sec^{-1}):

$-14.1 \pm 38.2j$, $-13.2 \pm 5.2j$, $-1.20 \pm 0.21j$, $+0.11 \pm 0.36j$, $+0.04 \pm 0.50j$

[a] $\dot{x} = Fx + Gu + \Gamma w$; $x^T = [\theta_R, \varphi_R, p_R, q_R, \theta_F, \varphi_F, q_F, p_F, u, v]$ $u^T = [\theta_c, \theta_s]$ = lateral, longitudinal cyclic pitch, $w^T = [u_w, v_w]$.

the following constant-coefficient linear model for the roll-pitch-horizontal translation motions (linearized about equilibrium hover):

$$\dot{x} = Fx + Gu + \Gamma w$$

where

$$x^T = (\theta_R, \varphi_R, q_R, p_R, \theta_F, \varphi_F, q_F, p_F, u, v) = \quad (1)$$

state vector

$$u^T = (\theta_c, \theta_s) = \text{control vector}$$

$$w^T = (u_w, v_w) = \text{horizontal wind vector}$$

and

$$q_R = \dot{\theta}_R, \; p_R = \dot{\varphi}_R, \; q_F = \dot{\theta}_F, \; p_F = \dot{\varphi}_F$$

(u,v) are velocity components of the mass center along the (x,y) fuselage axes. (θ_s,θ_c) are longitudinal and lateral cyclic pitch perturbations, respectively. A feedback controller, $\mathbf{u} = C\mathbf{x}$, was designed in Ref. 9 for this system, assuming perfect measurements of the ten vehicle state variables.

In Table 1, the elements of the 10 × 10 matrix F, the 10 × 2 matrices G and Γ, and the open-loop eigenvalues are given for a Sikorsky S-61 helicopter. For controls fixed ($\theta_s = \theta_c = 0$), the open-loop eigenvalues of this model are quite close to those of a model used by Sikorsky engineers.[9]

A Model that Assumes Instantaneous Rotor Tilting

Standard practice for helicopter autopilot design is to treat the aircraft as a single rigid body with "instantaneous" rotor tilting (i.e., to neglect the effects of rotor dynamics).[1,2] If the rotor dynamics are neglected for our example vehicle, the vehicle model reduces to sixth order and, by proper scaling, the cyclic pitch controls (θ_c,θ_s) become identical to the rotor tilt angles $(-\varphi_R,\theta_R)$. In Table 2, the elements of the 6 × 6 matrix F, the 6 × 2 matrix G, 6 × 2 matrix Γ, and the open-loop eigenvalues are given for the same vehicle that was modeled in Table 1 with rotor dynamics.

Table 2 Roll-pitch-horizontal velocity model of Sikorsky S-61 helicopter for instantaneous rotor tilting[a]

$$F = \begin{bmatrix} 0 & 0 & 1 & 0 & 0 & 0 \\ 0 & 0 & 0 & 1 & 0 & 0 \\ 0 & 0 & -0.415 & 0.318 & 0.00338 & 0.00116 \\ 0 & 0 & -1.23 & -1.58 & 0.00415 & -0.0124 \\ -32.2 & 0 & 4.70 & -1.02 & -0.0198 & -0.0059 \\ 0 & 32.2 & -1.02 & -4.70 & 0.0059 & -0.0198 \end{bmatrix}$$

$$G = \begin{bmatrix} 0 & 0 \\ 0 & 0 \\ -0.295 & 6.27 \\ -23.1 & -1.08 \\ 0.977 & -32.2 \\ -32.2 & -0.977 \end{bmatrix}$$

$$\Gamma = \begin{bmatrix} 0 & 0 \\ 0 & 0 \\ 0.00338 & 0.00116 \\ 0.00415 & -0.0124 \\ -0.0198 & -0.0059 \\ 0.0059 & -0.0198 \end{bmatrix}$$

Open loop eigenvalues are

$$(-1.2, -1.1, 0.11 \pm 0.36j, 0.04 \pm 0.50j) \; sec^{-1}$$

[a] $\dot{\mathbf{x}} = F\mathbf{x} + Gu + \Gamma\mathbf{w}$; $\mathbf{x}^T = [\theta_F, \varphi_F, q_F, p_F, u, v]$, $\mathbf{u}^T = [\theta_c, \theta_s]$, $\mathbf{w}^T = [u_w, v_w]$, (θ_c, θ_s) = (lateral, longitudinal) cyclic pitch $\cong (-\varphi_R, \theta_R)$ = (−roll, pitch) tilt angles of rotor. All units in ft, sec; angles in rad.

Table 3 Gains for controller I (with rotor feedback) and controller II (without rotor feedback) (units in ft, sec; angles in rad)

$$CI = \begin{bmatrix} 0.26 & 0.31 & 0.007 & -0.001 & 0.27 & 0.98 & 0.11 & 0.27 & 0.02 & -0.02 \\ -0.16 & 0.17 & 0.001 & 0.007 & -0.98 & 0.27 & -0.54 & 0.04 & -0.06 & -0.006 \end{bmatrix}$$

$$CII = \begin{bmatrix} 0 & 0 & 0 & 0 & 0.18 & 1.00 & 0.17 & 0.23 & 0.01 & -0.03 \\ 0 & 0 & 0 & 0 & -1.02 & 0.17 & -0.50 & 0.01 & -0.06 & -0.006 \end{bmatrix}$$

Table 4 Closed-loop eigenvalues using controllers I and II, $A_\theta = I$

Mode[a]	10th-order model with CI[b]	6th-order model with CII[b]	10th-order model with CII[b]
1.	$-14.1 \pm 38.2j$		$-15.2 \pm 36.2j$
2.	$-13.2 \pm 5.2j$		$-7.75 \pm 9.6j$
3.	$-3.60 \pm 3.40j$	$-3.56 \pm 3.34j$	$-4.68 \pm 1.76j$
4.	$-1.85 \pm 1.83j$	$-1.81 \pm 1.72j$	$-2.13 \pm 2.13j$
5.	$-0.06 \pm 0.007j$	$-0.06 \pm 0.008j$	$-0.05 \pm 0.008j$

[a]The mode identification is determined by the eigenvectors and corresponds to the eigenvalues which are: Mode 1) rotor nutation, 2) rotor precession, 3) fuselage pitch-roll, 4) fuselage pitch-roll, longitudinal velocity, and 5) fuselage pitch-roll-lateral velocity.
[b]Units are rad/sec.

Inclusion of Rotor Dynamics in Hover Autopilot Design for Tight Control

The justification for neglecting rotor dynamics is based on the large separation of the characteristic rotor frequencies from the characteristic fuselage rigid body frequencies, and the practical difficulty of measuring rotor tilt and tilt rate.

Demonstration of the need for including rotor states in a "tight" autopilot is made here by comparing the performance of two high gain controllers designed using OPTSYS. Controller I feeds back both the rotor states $(\theta_R,\varphi_R,q_R,p_R)$ and the fuselage states $(\theta_F,\varphi_F,q_F,p_F,u,v)$ while controller II feeds back only fuselage states. Both controllers are evaluated on the tenth order coupled rotor fuselage model of Table 1.

Controller I was designed, using the tenth order model of Table 1 that includes rotor dynamics, whereas controller II was designed using the sixth order model of Table 2 that assumes instantaneous rotor tilting. The quadratic performance index used was of the form

$$J = \frac{1}{2}\int_0^\infty [A_\theta(\theta_F^2 + \varphi_F^2) + A_u(u^2 + v^2) + \theta_c^2 + \theta_s^2]dt \quad (2)$$

For $A_\theta = 1$, $1/[(A_u)^{1/2}] = 660$ ft sec^{-1}, the state-feedback gains, C, are shown in Table 3, where

$$u = Cx \quad (3)$$

Table 4 shows the closed loop eigenvalues of the tenth order system with controllers I and II. For comparison, those of the 6th-order system with controller II are also given.

Although the closed loop eigenvalues for the tenth order model with controller CI differ slightly from those with controller CII, the lower order controller is satisfactory. Neglect of rotor dynamics is justified for this autopilot requirement.

Consider now the design of controllers which are to hold fuselage pitch and roll angles to smaller deviations. The technique is to increase the weighting factor, A_θ, on the fuselage pitch and roll angles from 1 (controllers I and II), to 10 (controllers I-a and II-a), and then to 100, (controllers I-b and II-b). These tighter controllers are then evaluated on the tenth order model. The gains of controller IIa and IIb are shown in Table 5.

Figure 2 shows a root-locus plot of the closed loop intermediate eigenvalues (modes 2,3) as A_θ is increased. Mode 2, the rotor precession mode, becomes unstable at high fuselage angle weighting if no rotor feedback is used.

It is concluded that such high gain, tight autopilots should include rotor state feedback to insure stability of rotor response. In the following discussion, attention is directed to determining rotor state from sensor measurements.

A Wind Model

The wind components (u_w,v_w) along the (x,y) fuselage axes are modeled by independent exponentially correlated Gauss-Markov processes.[10]

$$\begin{aligned} \dot{u}_w &= -(1/\tau_c)u_w + q_u \\ \dot{v}_w &= -(1/\tau_c)v_w + q_v \end{aligned} \quad (4)$$

where

$$E[q_u] = E[q_v] = 0, \; E\begin{bmatrix} q_u(t)q_u(t'), & q_u(t)q_v(t') \\ q_v(t)q_u(t'), & q_v(t)q_v(t') \end{bmatrix} = \begin{bmatrix} Q_w, & 0 \\ 0 & Q_w \end{bmatrix}\delta(t-t')$$

and

$$Q_w = 2\sigma_w^2/\tau_c$$

τ_c is the correlation time of the wind. In the statistical steady-state equation (4) gives $E[u_w] = E[v_w] = 0$, $E[u_w^2] = E[v_w^2] = \sigma_w^2$, $E[u_w v_w] = 0$. For the simulations here, we took $\tau_c = 3.2$ sec and $\sigma_w = 20$ ft sec^{-1}, which is a very strong, gusty wind.

Equation (4) is called a "shaping filter" for the wind; using this approach, u_w and v_w become additional (eleventh and twelfth) state variables of the system. The

Table 5 Gains for Controller II-a and Controller II-b

$$CIIa = \begin{bmatrix} 0 & 0 & 0 & 0 & 0.37 & 3.15 & 0.04 & 0.46 & 0.01 & -0.003^a \\ 0 & 0 & 0 & 0 & -3.16 & 0.37 & -0.93 & 0.02 & -0.05 & -0.02 \end{bmatrix}$$

$$CIIb = \begin{bmatrix} 0 & 0 & 0 & 0 & 0.88 & 9.97 & 0.08 & 0.87 & +0.001 & -0.02^b \\ 0 & 0 & 0 & 0 & -9.97 & 0.87 & -1.71 & 0.04 & -0.05 & -0.02 \end{bmatrix}$$

[a] These gains correspond to $A_\theta = 10$.
[b] These gains correspond to $A_\theta = 100$.

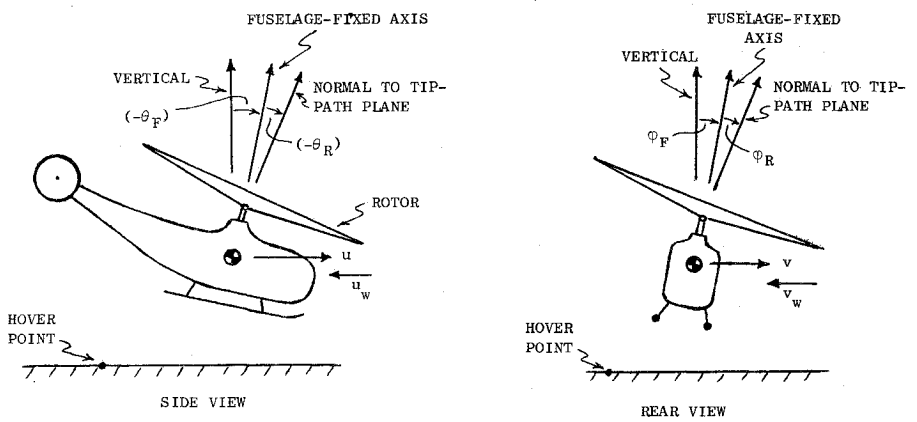

Fig. 1 Model reference axes.

augmented equations are then:

$$\underbrace{\begin{bmatrix} \dot{x} \\ \dot{u}_w \\ \dot{v}_w \end{bmatrix}}_{\dot{x}'} = \underbrace{\left[\begin{array}{c|cc} F & \multicolumn{2}{c}{\Gamma} \\ \hline 0 & -1/\tau_c & 0 \\ 0 & 0 & -1/\tau_c \end{array}\right]}_{F'} \underbrace{\begin{bmatrix} x \\ u_w \\ v_w \end{bmatrix}}_{x'} + \underbrace{\begin{bmatrix} G \\ 0 \\ 0 \end{bmatrix}}_{G'} u + \underbrace{\left[\begin{array}{cc} 0 & \\ \hline 1 & 0 \\ 0 & 1 \end{array}\right]}_{\Gamma'} q_w \tag{5}$$

The perfect-information-controller now contains four additional feedback gains on u_w and v_w

$$\begin{bmatrix} \theta_c \\ \theta_s \end{bmatrix} = Cx + C_w \begin{bmatrix} u_w \\ v_w \end{bmatrix} \tag{6}$$

The other twenty gains, C, are not changed by addition of these two state variables, since Eq. (4) is coupled only one-way to Eq. (1). In fact, the four additional gains, C_w, may be determined in terms of τ_c and the steady state Riccati matrix corresponds to Eq. (1) in Ref. 11. For the numerical values used here, the four additional gains are

$$C_w = \begin{bmatrix} 0.00021, & -0.00051 \\ -0.00050, & -0.00020 \end{bmatrix} \tag{7}$$

Sensor Error Models

Measurements of fuselage roll angle, φ_F, and fuselage pitch angle, θ_F, have been used for some time as basic inputs to autopilots. They are readily obtained from the vertical reference systems of the aircraft which usually consists of a two-degree-of-freedom gyro with two electrolytic bubble levels. We have assumed that these measurements contain additive white noise with zero mean. For one system we assumed a power spectral density of 2.8×10^{-6} rad^2 sec, which was estimated by considering an rms error of 0.22° with a correlation time of 0.1 sec. For another, more accurate, system, we assumed an rms error of 0.09°, still with a correlation time of 0.1 sec. Actually, vertical gyro measurements are sensitive to lateral accelerations since the bubble levels measure the "apparent vertical." Thus our white noise error model is really more appropriate to angle measurements from an inertial measurement unit (IMU) with a stable platform.

Measurements of the roll angle, φ_R, and the pitch angle, θ_R, of the rotor tip-path-plane are more difficult and more expensive. Direct rotor angle measurements for articulated rotors have been made with potentiometers or strain gauges on the blade flapping hinge. The principal drawback of this technique is the required resolution of the measurements from rotating to nonrotating axes. This complexity and the extra weight are justified mainly for flight tests and not for operational use. Other direct methods could be based on directly linking the blade tips to a shaft mounted sensor or on electromagnetic (possibly optical) techniques. For example, small electromagnetic radiators at the rotor tips could be detected at the hub by direction-sensitive receivers, two in pitch and two in roll.

Indirect rotor angle measurements have been made by sensing hub moments. The AH-56 helicopter originally used a shaft mounted gyro which was torqued by moments proportional to the hingeless blade flapping. The difficulties of this system lie in the added complexity, the poor drag characteristics of the gyro assembly, and in the problem of isolating the moment sensors from vibrations.

We have assumed that measurements of φ_R and θ_R contain additive white noise with zero mean, and we have considered two levels of power spectral density. One of these levels is high (7.1×10^{-6} rad^2 sec), corresponding to inaccurate measurements, and the other is low (7.1×10^{-8} rad^2 sec), corresponding to very accurate measurements. These levels were estimated by considering a correlation time of 0.1 sec and rms errors of 1.0° and 0.1°, respectively. The latter is probably more accurate than can be expected but serves to tell us whether or not an attempt to develop very accurate rotor sensors would be worthwhile in terms of improving vehicle response.

Filters to Estimate Vehicle States from Measurements of Fuselage Roll/Pitch Angles

Two steady-state Kalman filters corresponding to the twelfth order model of Eq. (5) were designed using OPT-

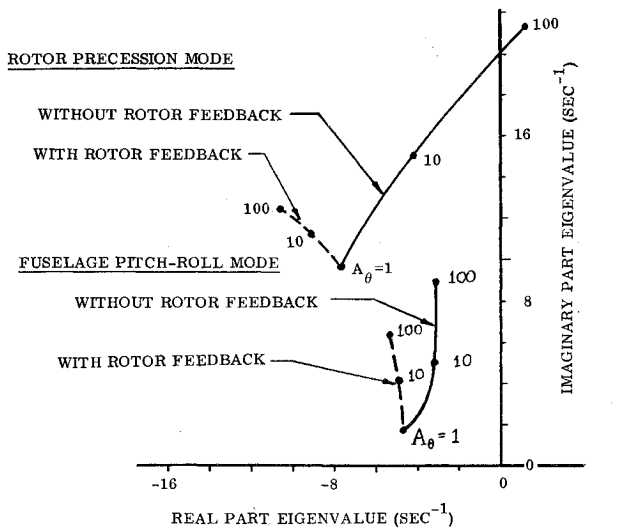

Fig. 2 Rotor precession and fuselage pitch-roll eigenvalues with and without rotor state feedback A_θ = 1, 10, 100.

Table 6 Gain matrices for filters A and B (all units in sec, ft; angles in rad)

Filter A—less accurate measurements

$$K^T = \begin{bmatrix} 2.58 & 0.12 & -3.02 & -0.80 & 5.75 & 0.10 & 16.90 & 0.22 & -86.1 & 5.35 & 7550. & 1320. \\ 0.37 & 1.47 & 1.80 & -6.54 & 0.10 & 8.44 & 1.15 & 35.60 & 2.89 & 37.10 & 1430. & -8060. \end{bmatrix}$$

Filter B—more accurate measurements

$$K^T = \begin{bmatrix} 7.60 & 0.71 & -7.40 & -2.08 & 8.0 & 0.20 & 32.3 & 2.0 & -172. & 3.56 & 19450. & 3360. \\ 0.19 & 5.36 & 3.30 & -17.8 & 0.20 & 11.92 & 1.91 & 71.3 & -2.82 & 89.4 & 3510. & -20500. \end{bmatrix}$$

Table 7 Eigenvalues (sec^{-1}) of estimate errors for filters A and B compared

Filter A	$-14.1 \pm 38.2j$	$-13.3 \pm 5.2j$	$-2.54 \pm 4.35j$	-1.62 ± 2.83	$-5.05, -3.40$	$-.0011^a$
Filter B	$-14.1 \pm 38.2j$	$-13.3 \pm 5.2j$	$-3.49 \pm 5.90j$	-2.13 ± 3.82	$-6.65, -4.62$	$-.00044^a$

[a] Double roots.

Table 8 The rms error in filter estimates for filters A and B (units in sec, ft; angles in deg)

	$\tilde{\theta}_R$	$\tilde{\varphi}_R$	$\tilde{q}_R$	$\tilde{p}_R$	$\tilde{\theta}_F$	$\tilde{\varphi}_F$	$\tilde{q}_F$	$\tilde{p}_F$	$\tilde{u}$	$\tilde{v}$	$\tilde{u}_w$	$\tilde{v}_w$
Filter A	0.27	0.18	1.63	1.65	0.23	0.28	0.85	1.44	1.65	1.65	10.7	9.9
Filter B	0.24	0.17	1.62	1.62	0.11	0.14	0.56	1.02	1.05	1.05	10.4	8.8

SYS for measurements of θ_F and φ_F, assumed to contain additive white noise. Numerical values for F' were obtained from Table 1 and below Eq. (4); two values for the power spectral density of the measurement noise were used, 2.8×10^{-6} rad^2 sec for Filter A, and 0.48×10^{-6} rad^2 sec for Filter B. The filters have the form

$$\dot{\hat{x}}' = F'\hat{x}' + G'u + K(z - H\hat{x}') \tag{8}$$

where

$$z = \begin{bmatrix} \theta_F + \text{noise} \\ \varphi_F + \text{noise} \end{bmatrix} = \text{measurements}$$

$$H = \begin{bmatrix} 0\ 0\ 0\ 0\ 1\ 0\ 0\ 0\ 0\ 0\ 0\ 0 \\ 0\ 0\ 0\ 0\ 0\ 1\ 0\ 0\ 0\ 0\ 0\ 0 \end{bmatrix}$$

$$(\hat{x}')^T = [\hat{\theta}_R, \hat{\varphi}_R, \hat{q}_R, \hat{p}_R, \hat{\theta}_F, \hat{\varphi}_F, \hat{q}_F, \hat{p}_F, \hat{u}, \hat{v}, \hat{u}_w, \hat{v}_w]$$

= estimates of the state variables

The gains, K, are given in Table 6. Some of the gains change sign in going from Filter A to Filter B. Such sign changes with measurement accuracy are not uncommon.

The eigenvalues of the filter error, $\tilde{\mathbf{x}}' = (\hat{\mathbf{x}}' - \mathbf{x}')$ are given in Table 7; they indicate the response decay of the error. The smallest eigenvalues are real and indicate rather slow error decay for that filter mode.

The rms values of the estimate errors are given in Table 8. These are the square roots of the diagonal terms of the error covariance matrix. The rotor estimate errors and the wind velocity errors are not significantly changed by increased fuselage measurement accuracy, but the fuselage estimate errors are substantially reduced.

Filters to Estimate Vehicle States from Measurements of Fuselage Roll/Pitch Angles and Rotor Roll/Pitch Angles

Two other steady-state Kalman filters were designed for the model of Eq. (5); these filters have four measurements as inputs, θ_R,φ_R,θ_F, and φ_F. Both filters assumed the less accurate fuselage angle measurements (noise power spectral density 2.8×10^{-6} rad^2 sec). Two values for the noise power spectral density of the rotor angle measurements were used, 7.1×10^{-6} rad^2 sec for Filter C, and 7.1×10^{-8} rad^2 sec for Filter D. The filters have the same form as Eq. (8) except that now

$$z = \begin{bmatrix} \theta_R + \text{noise} \\ \varphi_R + \text{noise} \\ \theta_F + \text{noise} \\ \varphi_F + \text{noise} \end{bmatrix} = \text{measurements}$$

$$H = \begin{bmatrix} 1\ 0\ 0\ 0\ 0\ 0\ 0\ 0\ 0\ 0\ 0\ 0 \\ 0\ 1\ 0\ 0\ 0\ 0\ 0\ 0\ 0\ 0\ 0\ 0 \\ 0\ 0\ 0\ 0\ 1\ 0\ 0\ 0\ 0\ 0\ 0\ 0 \\ 0\ 0\ 0\ 0\ 0\ 1\ 0\ 0\ 0\ 0\ 0\ 0 \end{bmatrix}$$

The gains K are given in Table 9, the eigenvalues of the error estimates, $\tilde{\mathbf{x}}' = \hat{\mathbf{x}}' - \mathbf{x}'$, are given in Table 10, and the rms errors of the estimates are given in Table 11.

Table 9 Gains for filters C and D (all units in sec, ft; angles in rad)

Filter C—less accurate rotor measurements

$$K^T = \begin{bmatrix} 1.99 & 0.13 & 2.28 & 3.82 & 0.47 & 0.08 & 3.68 & 0.17 & -5.10 & 0.86 & 4560. & 610. \\ 0.13 & 1.21 & -3.42 & 0.96 & 0.002 & 0.42 & 0.28 & 5.90 & -0.07 & -2.32 & 635. & -3160. \\ 1.16 & 0.006 & -1.62 & -0.50 & 4.51 & 0.01 & 10.5 & -0.26 & -66.5 & 3.38 & 3890. & 704. \\ 0.19 & 1.06 & 1.67 & -5.26 & 0.01 & 7.71 & 0.54 & 30.2 & 3.91 & 36.2 & 794. & -6650. \end{bmatrix}$$

Filter D—more accurate rotor measurements

$$K^T = \begin{bmatrix} 20.9 & 0.05 & 218. & 154. & 0.27 & 0.40 & 10.2 & 2.68 & 119.7 & -38.2 & 57000. & -9510. \\ 0.05 & 19.8 & -152. & 196. & -0.10 & 0.53 & -0.67 & 34.9 & -36.8 & -124. & -9510. & -56500. \\ 0.007 & 0.003 & -0.10 & -0.04 & 1.68 & -0.006 & 1.42 & -0.12 & -33.8 & 0.92 & 392. & 4.32 \\ 0.001 & 0.013 & 0.04 & -0.56 & -0.006 & 3.63 & 0.09 & 6.62 & 1.73 & 29.2 & -75.6 & -1117. \end{bmatrix}$$

Table 10 Eigenvalues (sec^{-1}) of estimate errors for filters C and D

Filter C	$-14.2 \pm 38.2j$	$-13.2 \pm 5.6j$	$-1.78 \pm 2.42j$	$-4.58 \pm 0.31j$	$-0.27 \pm 4.10j$	-0.0011^a
Filter D	$-15.0 \pm 41.5j$	$-22.2 \pm 1.21j$	$-12.1 \pm 10.9j$	$-1.49 \pm 1.42j$	$-0.76 \pm 0.74j$	-0.0011^a

[a] Double roots.

Table 11 The rms errors of estimates for filters C and D (units in ft, sec; angles in deg)

	$\tilde{\theta}_R$	$\tilde{\varphi}_R$	$\tilde{q}_R$	$\tilde{p}_R$	$\tilde{\theta}_F$	$\tilde{\varphi}_F$	$\tilde{q}_F$	$\tilde{p}_F$	$\tilde{u}$	$\tilde{v}$	$\tilde{u}_w$	$\tilde{v}_w$
Filter C	0.22	0.17	1.62	1.62	0.20	0.27	0.62	1.34	1.65	1.65	9.50	9.20
Filter D	0.06	0.07	1.43	1.40	0.13	0.19	0.12	0.44	1.65	1.65	4.95	5.10

Table 12 Predicted rms responses of vehicle to random wind using various filter/controllers (units in ft, sec; angles in deg)

	θ_R	φ_R	q_R	p_R	θ_F	φ_F	q_F	p_F	u	v	θ_c	θ_s
Filter A	0.69	0.59	7.21	7.62	0.71	0.73	1.28	2.30	3.15	2.69	0.89	0.95
Filter B	0.54	0.47	5.79	6.10	0.47	0.48	0.85	1.71	2.35	2.01	0.80	0.84
Filter C	0.53	0.53	6.06	6.78	0.55	0.66	0.85	2.13	2.67	2.56	0.85	0.84
Filter D	0.19	0.22	3.19	3.49	0.20	0.29	0.21	0.85	1.91	1.96	0.68	0.65
Perfect info.	0.08	0.08	0.16	0.19	0.05	0.05	0.04	0.04	0.84	0.82	0.65	0.65

Filter A—Less accurate fuselage measurements.
Filber B—More accurate fuselage measurements.
Filter C— Less accurate fuselage measurements and less accurate rotor measurements.
Filter D—Less accurate fuselage measurements and more accurate rotor measurements.
Perfect info.—Perfect measurements of all states (limiting, unrealistic case).
rms longitudinal and lateral winds 20 ft sec^{-1} with 3.2 sec correlation time.

A comparison of the rms errors of the estimates for Filter A (Table 8) with those of Filter C (Table 11) shows only a slight reduction by adding the less accurate rotor measurements.

When the more accurate rotor measurements are used (Filter D), significant changes in the eigenvalues of the estimate errors occur (Table 10). The gains on the rotor states for this Filter D are significantly increased (Table 9). Reduction of the rotor state estimate errors is accompanied by reduction of the fuselage angle and wind velocity estimate errors, but the velocity errors are not reduced at all (Table 11).

Mean Square Response of Controlled Vehicle to a Random Wind

Combining any one of the filters of Tables 6 or 9 with the feedback gains of the perfect information controller CI of Table 3, produces a dynamic compensator, shown schematically in Fig. 3.

The steady-state, mean-square response of the vehicle, $X = E(xx^T)$, using such an autopilot can be predicted by solving a set of $78 = (\frac{1}{2})(12)(13)$ linear equations for the elements of $\hat{X} = E(\hat{x}\hat{x}^T)$ and adding this matrix to $P = E(x - \hat{x})(x - \hat{x})^T$,§ i.e.,

$$X = \hat{X} + P \tag{9}$$

where

$$(F - GC)\hat{X} + \hat{X}(F - GC)^T = -KRK^T \tag{10}$$

§See, e.g., Ref. 12, pp. 416–418.

and F' is the augmented (12 × 12) open-loop dynamics matrix, G' is the augmented (12 × 2) control distribution matrix, C' is the augmented (2 × 12) feedback gain matrix, K' is the augmented filter gain matrix (12 × 2 or 12 × 4), R is the measurement error power spectral density matrix = $E(z - Hx)(z - Hx)^T$, and P is the covariance matrix of the estimate error. In addition, the steady-state mean-square control activity can be predicted from

$$E(uu^T) = C\hat{X}C^T \tag{11}$$

These computations were done using OPTSYS[4] computer program and the root-mean-square (rms) responses of the ten vehicle states and the two controls¶ are shown in Table 12 for autopilots using Filters A, B, C, and D. For comparison the rms responses of the perfect information controller are also shown in Table 12; in this latter case, we assume perfect measurements of all state vari-

¶These are the square roots of the diagonal elements of X and $E(uu^T)$.

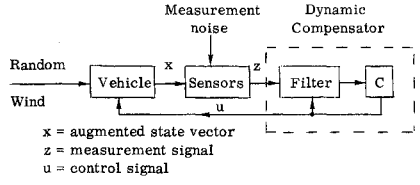

Fig. 3 Block diagram of filter-controller as a dynamic compensator.

ables; and the mean square response is obtained from

$$(F - GC)X + X(F - GC)^T = -\Gamma Q_w \Gamma^T \tag{12}$$

$$E(uu^T) = CXC^T \tag{13}$$

where Γ is defined in Eq. (5), and Q_w = power spectal density of q_w, defined in Eq. (4).

As expected, the rms responses are smallest when perfect information on all states is fed back; however, this is an idealized situation we can never realize. Using Filter A in the autopilot (the less accurate measurements of fuselage roll/pitch angles) still produces surprisingly small responses to such a strong, gusty lateral wind.

Using Filter B in the autopilot (the more accurate measurements of fuselage roll/pitch angles) shows some reduction in rms responses over the use of Filter A, as expected. The interesting point is that this system is better than the system using Filter C which uses the less accurate measurements of both fuselage and rotor roll/pitch angles. In other words, Filter B estimates the rotor states more accurately than they are measured for Filter C!

Filter D uses limiting, almost unattainably accurate measurements of rotor pitch and roll angles along with the less accurate measurements of fuselage pitch and roll angles. Using Filter D in the autopilot produces a substantial improvement in rms response over the use of Filter A.

Conclusions

A simplified model of a large helicopter has been used to investigate hover autopilot design concepts. Since the example aircraft is typical of helicopters for which hovering is a specific requirement, the following conclusions were reached: Including rotor dynamics in controller design for rotary-wing VTOL aircraft improves vehicle performance, particularly if precise pitch-roll requirements are to be met. The rotor states themselves need not be measured, since they can be estimated sufficiently accurately from fuselage measurements.

The techniques developed and discussed in this paper are applicable to other rotary-wing VTOL aircraft hover controllers. The extension to fully converted tilt rotor controllers, where gust sensitivity is an important concern, looks attractive.

References

[1]Murphy, R. D. and Narendra, K. S., "Design of Helicopter Stabilization Systems Using Optimal Control Theory," *Journal of Aircraft*, Vol. 6, No. 2, March–April 1969, pp. 129–126.

[2]Crossley, T. R. and Porter, B., "Synthesis of Helicopter Stabilization Systems Using Modal Control Theory," *Journal of Aircraft*, Vol. 9, No. 1, Jan. 1972, pp. 3–8.

[3]Kalman, R. E. and Englar, T. S., "A User's Manual for the Automatic Synthesis Program," CR-475, June 1966, NASA.

[4]Bryson, A. E. and Hall, W. E., "Optimal Control and Filter Synthesis by Eigenvector Decomposition," SUDAAR 436, Dec. 1971, Stanford Univ., Stanford, Calif.

[5]MacFarlane, A. G. J., "An Eigenvector Solution of the Linear Optimal Regulator Problem," *Journal of Electronics and Control*, Vol. 14, June 1963, pp. 643–654.

[6]Potter, J. E., "Matrix Quadratic Solutions," *SIAM Journal of Applied Mathematics*, Vol. 14, No. 3, May 1966, pp. 496–501.

[7]Francis, J. G. F., "The QR Transformation," *Computer Journal*, Vol. 4, No. 3, Pt. I, Oct. 1961, pp. 265–271; Vol. 4, No. 4, Pt. II, Feb. 1962, pp. 332–345.

[8]Hall, W. E., "Computational Methods for the Synthesis of Rotary-Wing VTOL Aircraft Control Systems," Ph.D. dissertation, Aug. 1971, Stanford Univ., Stanford, Calif.

[9]Bryson, A. E., Chasteen, L. H., Hall, W. E., and Mohr, R. L., "Studies of Control and Guidance for Rotary Wing VTOL Vehicles," SUDAAR 419, March 1971, Stanford Univ., Stanford, Calif.

[10]Miller, D. P. and Vinje, E. W., "Fixed Based Flight Simulation Studies of VTOL Aircraft Handling Qualities in Hovering and Low-Speed Flight," TR 67-152, Jan. 1968, Air Force Flight Dynamics Lab., Wright-Patterson Air Force Base, Ohio.

[11]Hall, W. E. and Bryson, A. E., "Synthesis of Hover Autopilots for Rotary-Wing VTOL Aircraft," SUDAAR 446, June 1972, Stanford Univ., Stanford, Calif.

[12]Bryson, A. E. and Ho, Y. C., *Applied Optimal Control*, Xerox-Blaisdell, Lexington, Mass., 1969.